The Astrophysical Journal, 685: L157–L160, 2008 October 1

FIRST RESULTS FROM THE TAIWANESE-AMERICAN OCCULTATION SURVEY (TAOS)

Z.-W. Zhang,[1] F. B. Bianco,[2,3] M. J. Lehner,[4,3] N. K. Coehlo,[5] J.-H. Wang,[1,4] S. Mondal,[1] C. Alcock,[3] T. Axelrod,[6] Y.-I. Byun,[7] W. P. Chen,[1] K. H. Cook,[8] R. Dave,[9] I. de Pater,[10] R. Porrata,[10] D.-W. Kim,[7] S.-K. King,[4] T. Lee,[4] H.-C. Lin,[1] J. J. Lissauer,[11] S. L. Marshall,[12,8] P. Protopapas,[3] J. A. Rice,[5] M. E. Schwamb,[13] S.-Y. Wang,[4] and C.-Y. Wen[4]

Received 2008 March 24; accepted 2008 August 21; published 2008 September 9

ABSTRACT

Results from the first 2 years of data from the Taiwanese-American Occultation Survey (TAOS) are presented. Stars have been monitored photometrically at 4 or 5 Hz to search for occultations by small (~3 km) Kuiper Belt objects (KBOs). No statistically significant events were found, allowing us to present an upper bound to the size distribution of KBOs with diameters 0.5 km $< D <$ 28 km.

Subject headings: Kuiper Belt — occultations — solar system: formation

1. INTRODUCTION

The study of the Kuiper Belt has exploded since the discovery of 1992 QB1 by Jewitt & Luu (1993). The brightness distribution of objects with R magnitude brighter than ~26 is relatively well established by many surveys, most recently by Fraser et al. (2008) and references therein. The brightness distribution is adequately described by a simple cumulative luminosity function $\Sigma(< R) = 10^{\alpha(R-R_0)}$ deg^{-2}, where $R_0 \sim 23$ and $\alpha \sim 0.6$, for objects with magnitude $R < 26$. There is clear evidence for a break to a shallower slope for fainter objects: the deepest survey, conducted using the Advanced Camera for Surveys on the *Hubble Space Telescope* (Bernstein et al. 2004), extended to $R = 28.5$, and found a factor of ~25 fewer objects than would be expected if the same distribution extended into this range.

The size distribution of Kuiper Belt objects (KBOs) is believed to reflect a history of *agglomeration* during the planetary formation epoch, when relative velocities between particles were low and collisions typically resulted in particles sticking together, followed by *destructive collisions* when the relative velocities were increased by dynamical processes after the giant planets formed (Stern 1996; Davis & Farinella 1997; Stern & Colwell 1997; Kenyon & Luu 1999a, 1999b; Kenyon & Bromley 2004; Pan & Sari 2005). The slope of the distribution function for larger objects reflects the early phase of agglomeration, while the shallower distribution for smaller objects reflects a subsequent phase of destructive collisions. The location of the break moves to larger sizes with time, while the distribution for smaller objects is expected to evolve toward a steady state collisional cascade (Kenyon & Bromley 2004; Pan & Sari 2005). Models for the spectrum of small bodies differ between Pan & Sari (2005) who derived a double-power-law distribution, and Kenyon & Bromley (2004) whose simulations show more structure, depending on material properties.

Thus, the size spectrum encodes information about the history of planet formation and dynamics. However, the size spectrum for small KBOs is not constrained by the imaging surveys because the objects of interest are too faint for direct detection using presently available instruments. These small objects may, however, be detected indirectly when they pass between an observer and a distant star (Bailey 1976; Dyson 1992; Axelrod et al. 1992; Brown & Webster 1997; Roques & Moncuquet 2000; Cooray & Farmer 2003; Nihei et al. 2007). The challenge confronting any survey exploiting this technique is the combination of very low anticipated event rate and short duration of the events (typically <1 s).

Other groups are attempting similar occultation surveys. Roques et al. (2006) reported three events in 10 star-hours of photometric data sampled at 45 Hz, which they modeled as objects at 15, 140, and 210 AU, respectively, placing the inferred objects outside the Kuiper Belt. Bickerton et al. (2008) reported results of 5 star-hours of data sampled at 40 Hz, during which no events were detected. Chang et al. (2006) reported a surprisingly high rate of possible occultation events in *RXTE* X-ray observations of Sco X-1, but many of these events have since been attributed to instrumental effects (Jones et al. 2008; Chang et al. 2007).

We report here the first results of the Taiwanese American Occultation Survey (TAOS). TAOS differs from the previously reported projects primarily in the extent of the photometric time series, a total of 1.53×10^5 star-hours, and in that data are collected simultaneously with three telescopes. Some compromises have been made in regard to the signal-to-noise ratio (S/N), which is typically lower than in previously reported surveys, and in cadence, which is 4 or 5 Hz, in contrast with the higher rates mentioned above. The substantial increase in exposure more than compensates for the lower cadence and S/N, and we are able to

[1] Institute of Astronomy, National Central University, No. 300, Jhongda Road, Jhongli City, Taoyuan County 320, Taiwan; s1249001@cc.ncu.edu.tw.
[2] Department of Physics and Astronomy, University of Pennsylvania, 209 South 33rd Street, Philadelphia, PA 19104.
[3] Harvard-Smithsonian Center for Astrophysics, 60 Garden Street, Cambridge, MA 02138.
[4] Institute of Astronomy and Astrophysics, Academia Sinica, P.O. Box 23-141, Taipei 106, Taiwan.
[5] Department of Statistics, University of California, 367 Evans Hall, Berkeley, CA 94720.
[6] Steward Observatory, 933 North Cherry Avenue, Room N204, Tucson, AZ 85721.
[7] Department of Astronomy, Yonsei University, 134 Shinchon, Seoul 120-749, Korea.
[8] Institute of Geophysics and Planetary Physics, Lawrence Livermore National Laboratory, Livermore, CA 94550.
[9] Initiative in Innovative Computing, Harvard University, 60 Oxford Street, Cambridge, MA 02138.
[10] Department of Astronomy, University of California, 601 Campbell Hall, Berkeley, CA 94720.
[11] Space Science and Astrobiology Division 245-3, NASA Ames Research Center, Moffett Field, CA 94035.
[12] Kavli Institute for Particle Astrophysics and Cosmology, 2575 Sand Hill Road, MS 29, Menlo Park, CA 94025.
[13] Division of Geological and Planetary Sciences, California Institute of Technology, 1201 East California Boulevard, Pasadena, CA 91125.

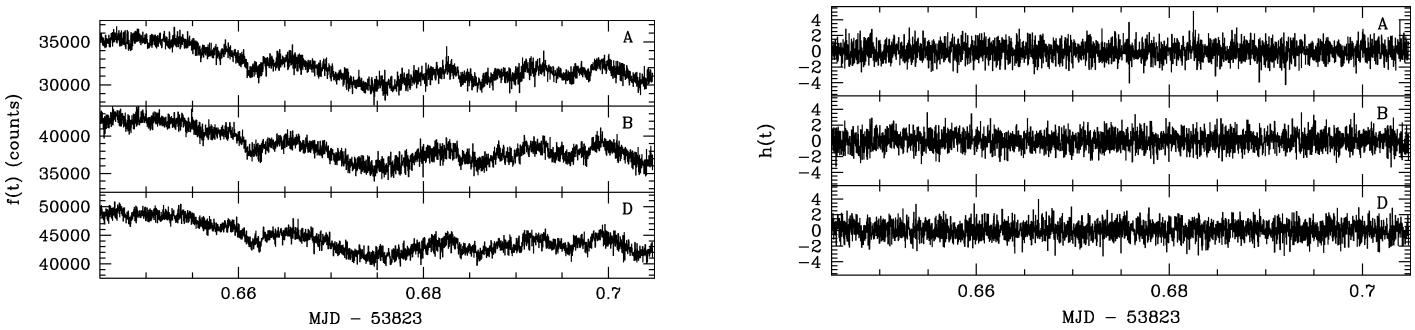

FIG. 1.—Demonstration of detrending by the filtering process. The left panel shows a raw light curve set $f(t)$, and the right panel shows the light curve set $h(t)$ after filtering. The total number points in the light curve set is 26,622, corresponding to 89 minutes. Here only one of every 10 points is plotted, for readability.

probe significant ranges of the model space for small KBOs. We have also developed a statistical analysis technique which allows efficient use of the multitelescope data to detect brief occultation events that would be statistically insignificant if observed with only one telescope.

2. DATA AND ANALYSIS

TAOS has been collecting scientific data since 2005. Observations are normally carried out simultaneously with three 50 cm telescopes (A, B, and D, separated by distances of 6 m and 60 m; this system is described by Lehner et al. 2008). Over 15 TB of raw images have been taken. We report here on the first 2 years of data taken simultaneously with all three telescopes. The data set comprises 156 *data runs*, where a data run is defined as a series of three-telescope observations of a given field for durations of ~90 minutes. Thirty data runs with a 4 Hz sampling rate were taken before 2005 December 15, and 126 data runs were collected subsequently with a sampling rate of 5 Hz. Only fields with ecliptic latitudes $|b| < 10°$ were analyzed. Over 93% of the data were collected in fields with $|b| < 3°$, so the results of our analysis are relevant to the sum of the cold and excited KBO populations (Bernstein et al. 2004). No data run was included unless each star was sampled more than 10,000 times in each telescope. The angle from opposition in these data runs is distributed from 0° to 90°. The number of stars (with $R < 13.5$, which typically gives a S/N ≥ 5) monitored in the data runs ranges between 200 and 2000.[14]

The images were analyzed using an aperture photometry package (Z.-W. Zhang et al. 2008, in preparation) devised exclusively for TAOS images. Light curves were produced for each star by assembling the photometric information into a time series. A star in each data run has a light curve from each of the three telescopes. The data presented in this Letter comprise 110,895 *light curve sets* (where a light curve set is defined as a set of three light curves, one for each telescope, for the same star in a single data run), containing 7.1×10^9 individual photometric measurements.

[14] Information on the TAOS fields is available at http://taos.asiaa.sinica.edu.tw/taosfield/.

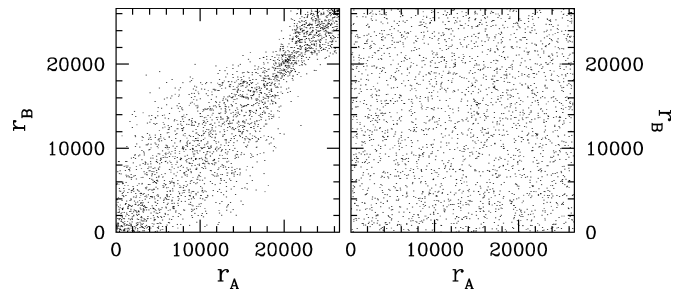

FIG. 2.—Rank-rank plots of the light curve set shown in Fig. 1. Each point shows the ranks at a single time point for telescopes A and B. The ranks from the raw light curves (Fig. 1, *left*) are shown in the left panel, and the ranks from the filtered light curves (Fig. 1, *right*) are shown in the right panel.

The photometric data are not calibrated to a standard system. Changes in atmospheric transparency during a data run produce flux variations (Fig. 1) that could undermine our occultation search algorithm. Such low-frequency trends in a light curve can be removed by a numerical high-pass filter that preserves information of a brief occultation event, typically with a duration less than 1–2 data points with the TAOS sampling rate. Our filter takes a time series of f_i measured at time t_i to produce an intermediate series $g_i = f_i - \bar{f}_i$ where $\bar{f}_i$ is the running average of 33 data points centered on t_i. The series g_i is then scaled by the local fluctuation, $h_i = g_i/\sigma(g_i)$ with $\sigma(g_i)$ being the standard deviation of g_i of 151 data points centered at t_i. Both the mean and standard deviation are calculated using *3 σ clipping*. This filtering proves effective to remove slow-varying trends in the light curve, while preserving high-frequency fluctuations that we aim to detect, as illustrated in Figure 1.

We now confront the two central challenges in the search for extremely rare occultation events in these data: (1) *to search for events simultaneously in three parallel data streams*, and (2) *to determine the statistical significance of any rare events that are found*. The second is not straightforward because the statistical distribution of our photometric measurements is not known in advance; approximations based on Gaussian statistics are unreliable far from the mean. This motivates a nonparametric approach.

We thus found it useful to represent each data point by its *rank* in the filtered, rescaled light curve data h_i. That is, the rank of a data point ranges from $r = 1$ (lowest h) to $r = N_P$ (highest h), for a data run comprising N_P photometric measurements taken with telescope A, B, or D. The *rank triples* (r_i^A, r_i^B, r_i^D) form the basis of further analysis of the multitelescope data. The statistical distribution of these ranks is known exactly, since each rank must occur exactly once in each time series. Thus, the probability that a given rank will occur at time t_i is $P(r_i) = 1/N_P$. When the photometric data are uncorrelated, the probability that a particular rank triple will occur is simply $P(r_i^A, r_i^B, r_i^D) = 1/N_P^3$. This allows a straightforward test for correlation between the photometric data taken in the three telescopes: the rank triples should be distributed uniformly in a cube with sides of length N_P. A nonuniform pattern in the cube, on the other hand, indicates correlation. Figure 2 shows an example of the rank series of one telescope

against another; this indicates that the raw photometric data f_i are strongly correlated, but the filtered data h_i are not.

Given that the rank triples are uncorrelated, the ranks can be used to search for possible occultation events, as follows: *A true occultation event will exhibit anomalous, correlated low ranks in all three telescopes*. The rank triples thus allow an elegant test for the statistical significance of a candidate event. Consider the quantity

$$\eta_i = -\ln (r_i^A r_i^B r_i^D / N_P^3).$$

Since the ranks are uncorrelated (unless we have an occultation event), we can calculate the exact probability density function[15] for η. This in turn allows us to compute the probability that a given triple of low ranks randomly occurred in an uncorrelated light curve set; this is our measure of statistical significance. An illustration of the power of this approach is shown in Figure 3, where a simulated occultation event is readily recovered.[16]

We thus screened all of our series of rank triples for events with low ranks in all three telescopes. In the analysis reported here, we considered only events for which $P(\eta \geq c) \leq 10^{-10}$, which leads to an expected value of 0.24 false positive events in the entire data set of 2.4×10^9 rank triples. *No statistically significant events emerged from this analysis*.[17]

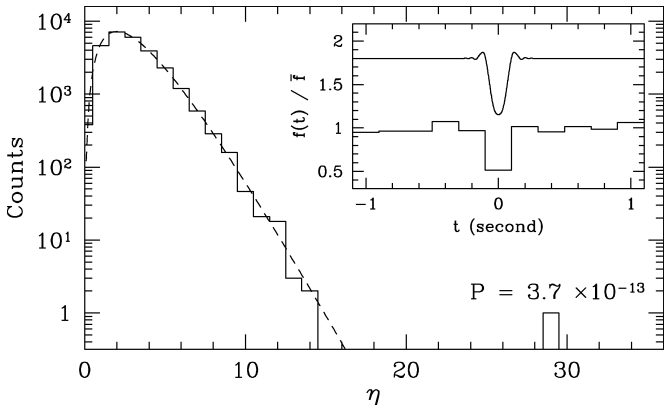

FIG. 3.—Histogram of η for a light curve set implanted with a *simulated* occultation by a 3 km KBO. Each light curve comprises 26,637 points and the ranks from the three telescopes are found to be 1, 3, and 1. The event is clearly visible at $\eta = 29.47$, and the probability of a rank product of 3 or lower from random chance is $P = 3.7 \times 10^{-13}$. The overlaid dashed line is the theoretical distribution of η. The theoretical and implanted light curves are shown in the inset, offset vertically for clarity.

3. EFFICIENCY TEST AND EVENT RATE

While the example event shown in Figure 3 is readily recovered, objects with smaller diameters or which do not directly cross the line of sight might not be so easily detected. An efficiency calculation is thus necessary for understanding the detection sensitivity of our data and analysis pipeline to different event parameters, notably the KBO size distribution. Our efficiency test started with implanting synthetic events into observed light curves, with the original noise. Each original light curve f_i was modified by the implanted occultation, $k_i = f_i - (1 - d_i)\bar{f}_i$, where d_i is the simulated event light curve (with baseline $d_i \rightarrow 1$ far from the event; Nihei et al. 2007), and $\bar{f}_i$ is the average of the original series over a 33 point rolling window. Since we preserved the original noise in the modified light curves, the noise where the implanted occultation event takes place—for which the flux diminishes—would be slightly overestimated; hence our efficiency estimate is conservative.

We assumed spherical KBOs at a fixed geocentric distance of $\Delta = 43$ AU. (Given our sampling rate, varying the KBO distance within the Kuiper Belt has little effect on our simulated light curves.) The event epoch t_0 was chosen randomly and uniformly within the duration E of the light curve set. The angular size θ_* of each star, necessary for the simulated light curve calculation, was estimated using stellar color and apparent magnitude taken from the USNO-B (Monet et al. 2003) and 2MASS (Skrutskie et al. 2006) catalogs. The impact parameter of each event was chosen, again randomly and uniformly, between 0 and $H/2$, where H is the *event cross section* (Nihei et al. 2007),

$$H = 2[(\sqrt{3}F)^{3/2} + (D/2)^{3/2}]^{2/3} + \theta_* \Delta.$$

Here D is the diameter of the occulting object, and F is the *Fresnel scale*, $F = (\lambda\Delta/2)^{1/2}$, where $\lambda = 600$ nm is the median wavelength in the TAOS filter. The relative velocity between the Earth and KBO $v_{\rm rel}$, necessary for the conversion of the occultation diffraction pattern to a temporally sampled light curve, is calculated based on the angle from opposition during each data run.

To adequately cover a wide range of parameter space, two efficiency runs were completed in which we implanted each light curve set with exactly one simulated occultation event. For each event, the diameter of the KBO was chosen randomly according to a probability, or weighting factor, w_D. In the first run, objects of diameters $D = 0.4$, 0.5, 0.6, 0.7, 0.8, and 0.9 km were added with $w_D = 1/6$ for each diameter. In the second run, objects of diameters $D = 1$, 2, 3, 5, 10 and 30 km were added with weights $w_D = \{100, 100, 100, 30, 5, 1\}/336$. The modified light curves k_i were reprocessed using the same procedure described in § 2. The recovered events and the event parameters were then used to calculate the number of expected occultation event in our survey. That is, we calculated the quantity

$$\Omega_e(D) = w_D^{-1} \sum_j [E_j v_{{\rm rel}_j} H_j(D)/\Delta^2],$$

where the sum is over all light curve sets where a simulated event is successfully recovered in the reanalysis (Fig. 4). Essentially $\Omega_e(D)$ is the *effective solid angle* of our survey, insofar as TAOS can be considered equivalent to a survey that is capable of counting every KBO of diameter D in a solid angle Ω_e with 100% efficiency.

The expected number of detected events by KBOs with sizes ranging from D_1 to D_2 can then be written as

$$N_{\rm exp} = \int_{D_2}^{D_1} \frac{dn}{dD} \Omega_e(D) dD, \quad (1)$$

[15] For small η, this distribution can be approximated by a Γ distribution of the form $P(\eta) = \eta^{N_T - 1} e^{-\eta}/(N_T - 1)!$, where $N_T = 3$ is the number of telescopes.

[16] Details of our statistical methodology will be described in M. J. Lehner et al. (2008, in preparation).

[17] A candidate event was reported in Chen et al. (2007). This event had a significance of 3.7×10^{-10}, which did not pass our cut on η. We expect to have ~1 false positive event at that significance level or higher.

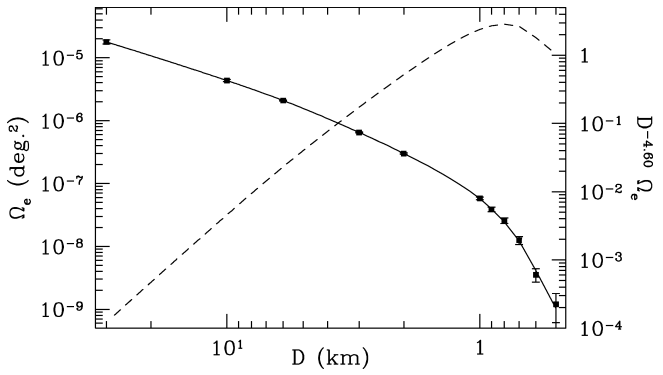

FIG. 4.—Effective solid angle of the TAOS survey as a function of KBO diameter D (*solid line*), and the product of the upper limit of the differential surface density by the effective solid angle (*dashed line*, in arbitrary units).

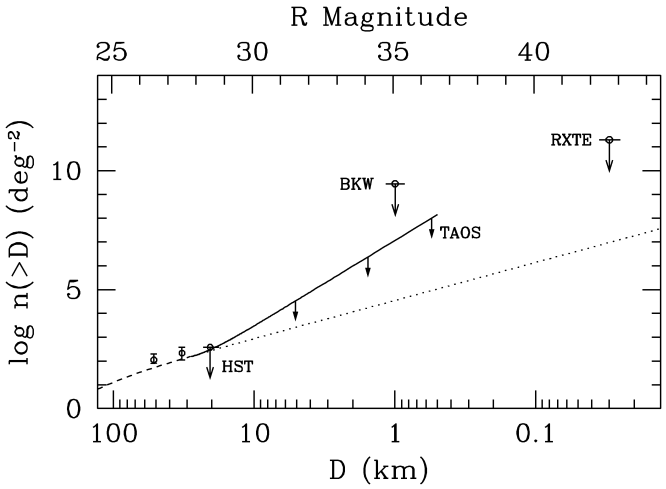

FIG. 5.—TAOS upper limit to the size spectrum (*solid line*) assuming a power-law distribution; double-power-law fit from Bernstein et al. (2004) (*dashed line*; extrapolation at $D < 28$ km shown with dotted line). Results from Bernstein et al. (2004) are shown as data points. Upper limits from Bickerton et al. (2008) (BKW) and Jones et al. (2008) (RXTE) are also shown. An albedo of 4% is assumed for computing magnitude.

where dn/dD is the differential surface number density of KBOs. The integrand of equation (1) contains two factors: the *model-dependent* size distribution dn/dD, and the *model-independent* effective solid angle $\Omega_e(D)$, which describes the sensitivity of the survey to objects of diameter D. Given the observed number of events and the value of $\Omega_e(D)$ resulting from the efficiency calculation, we can place model-dependent limits on the population of KBOs. Based on the absence of detections in this data set, any model with a size distribution such that $N_{\rm exp} \geq 3.0$ is inconsistent with our data at the 95% confidence level.

Note that there are an infinite number of models that satisfy the above requirement. We thus make the reasonable choice of a power-law size distribution $dn/dD = n_{\rm B}(D/28\ {\rm km})^{-q}$, where $n_{\rm B}$ is chosen such that the cumulative size distribution is continuous at 28 km with the results of Bernstein et al. (2004). We integrate equation (1) from $D_2 = 28$ km down to our detection limit of $D_1 = 0.5$ km, and solve equation (1) with $N_{\rm exp} = 3$, to find $q = 4.60$. Our null detection thus eliminates any power-law size distribution with $q > 4.60$ at the 95% c.l., setting a stringent upper limit (see Fig. 5) to the number density of KBOs.

4. CONCLUSION

We have surveyed the sky for occultations by small KBOs using the three telescope TAOS system. We have demonstrated that a dedicated occultation survey using an array of small telescopes, an innovative statistical analysis of multitelescope data, and a large number of star-hours, can be used as a powerful probe of small objects in the Kuiper Belt, and we are thus able to place the strongest upper bound to date on the number of KBOs with 0.5 km $< D <$ 28 km. We continue to operate TAOS, soon with an additional telescope, and will report more sensitive survey results in the future.

Work at NCU was supported by the grant NSC 96-2112-M-008-024-MY3. Work at the CfA was supported in part by the NSF under grant AST 05-01681 and by NASA under grant NNG04G113G. Work at ASIAA was supported in part by the thematic research program AS-88-TP-A02. Work at UCB was supported by the NSF under grant DMS-0405777. Work at Yonsei was supported by the KRCF grant to Korea Astronomy and Space Science Institute. Work at LLNL was performed under the auspices of the US DOE in part under contract W-7405-Eng-48 and contract DE-AC52-07NA27344. Work at SLAC was performed under US DOE contract DE-AC02-76SF00515. Work at NASA Ames was funded by NASA/PG&G.

REFERENCES

Axelrod, T. S., et al. 1992, in ASP Conf. Ser. 34, Robotic Telescopes in the 1990s, ed. A. V. Filippenko (San Francisco: ASP), 171
Bailey, M. E. 1976, Nature, 259, 290
Bernstein, G. M., et al. 2004, AJ, 128, 1364
Bickerton, S. J., Kavelaars, J. J., & Welch, D. L. 2008, AJ, 135, 1039
Brown, M. J. I., & Webster, R. L. 1997, MNRAS, 289, 783
Chang, H.-K., et al. 2006, Nature, 442, 660
———. 2007, MNRAS, 378, 1287
Chen, W. P., et al. 2007, in IAU Symp. 236, Near Earth Objects, Our Celestial Neighbors: Opportunity and Risk, ed. G. B. Valsecchi & D. Vokrouhlický (Cambridge: Cambridge Univ. Press), 65
Cooray, A., & Farmer, A. J. 2003, ApJ, 587, L125
Davis, D. R., & Farinella, P. 1997, Icarus, 125, 50
Dyson, F. J. 1992, QJRAS, 33, 45
Fraser, W. C., et al. 2008, Icarus, 195, 827
Jewitt, D., & Luu, J. 1993, Nature, 362, 730
Jones, T. A., Levine, A. M., Morgan, E. H., & Rappaport, S. 2008, ApJ, 677, 1241
Kenyon, S. J., & Bromley, B. C. 2004, AJ, 128, 1916
Kenyon, S. J., & Luu, J. X. 1999a, AJ, 118, 1101
———. 1999b, ApJ, 526, 465
Lehner, M. J., et al. 2008, PASP, submitted (arXiv:0802.0303)
Monet, D. G., et al. 2003, AJ, 125, 984
Nihei, T. C., et al. 2007, AJ, 134, 1596
Pan, M., & Sari, R. 2005, Icarus, 173, 342
Roques, F., & Moncuquet, M. 2000, Icarus, 147, 530
Roques, F., et al. 2006, AJ, 132, 819
Skrutskie, M. F., et al. 2006, AJ, 131, 1163
Stern, S. A. 1996, AJ, 112, 1203
Stern, S. A., & Colwell, J. E. 1997, AJ, 114, 841